Jurnal Penelitian dan Pengkajian Ilmu Pendidikan: e-Saintika
https://journal-center.litpam.com/index.php/e-Saintika/index

March 2026 Vol. 10, No. 1
e-ISSN: 2615-6881
pp. 195-213

Pseudo-Second-Order Kinetics of Ultrasound-Assisted Antioxidant Extraction from Mangosteen Peel Using a NaDES–VCO–Ethanol Solvent

***Jusman, Moh. Mirzan, Ahmad Ridhay, Citra Risty Andini, Novrita A. Sangkala, Siti Nur Aisyah**

Department of Chemistry, Faculty of Mathematics and Natural Sciences, Tadulako University, Palu, Central Sulawesi 94117, Indonesia.

*Corresponding Author e-mail: jusman_palu04@yahoo.com

Received: October 2025; Revised: March 2026; Published: March 2026

Abstract

Mangosteen peel is a rich source of xanthones and polyphenols with high antioxidant potential, but their efficient recovery requires extraction systems that are both effective and environmentally sustainable. In this study, ultrasound-assisted extraction (UAE) was combined with a hybrid green solvent consisting of natural deep eutectic solvents (NaDES), virgin coconut oil, and ethanol (VCO:EtOH = 1:1). A full 3 × 3 × 3 factorial design (27 runs) was used to evaluate the effects of NaDES concentration (30–50%), temperature (30–50 °C), and ultrasound amplitude (60–100%) on extraction yield and antioxidant activity measured by DPPH inhibition. Extraction kinetics were fitted using a nonlinear pseudo-second-order (PSO) model. The highest 60-min extraction yield was obtained at 50% NaDES, 50 °C, and 100% amplitude, reaching 26.2 ± 0.4% (n = 3), with DPPH inhibition of 94.4 ± 0.8% (n = 3). Under the same condition, the PSO model estimated an equilibrium yield (q_e) of 26.78%, with an RMSE of 0.067. Across all treatments, RMSE values ranged from 0.011 to 0.688, and extraction yield generally approached a plateau within 45–60 min. Yield was strongly and positively correlated with antioxidant activity ($r = 0.876$; 95% CI: 0.79–0.93; $p < 0.01$). These findings show that integrating UAE, a NaDES-based hybrid solvent, and PSO kinetic modeling can improve extraction efficiency and antioxidant performance while providing a reproducible framework for mangosteen peel valorization in nutraceutical and functional-food applications.

Keywords: Ultrasound-Assisted Extraction; Natural Deep Eutectic Solvents; Mangosteen Peel; Pseudo-Second-Order Kinetics; Antioxidant Activity; Green Extraction

How to Cite: Jusman, J., Mirzan, M., Ridhay, A., Andini, C. R., Sangkala, N. A., & Aisyah, S. N. (2026). Pseudo-Second-Order Kinetics of Ultrasound-Assisted Antioxidant Extraction from Mangosteen Peel Using a NaDES–VCO–Ethanol Solvent. *Jurnal Penelitian Dan Pengkajian Ilmu Pendidikan: E-Saintika*, *10*(1), 195-213. https://doi.org/10.36312/e-saintika.v10i1.3401

10.36312/e-saintika.v10i1.3401

INTRODUCTION

Mangosteen (Garcinia mangostana L.) is a tropical fruit widely cultivated in Southeast Asia and valued for its high content of bioactive compounds. Its peel, which represents more than half of the fruit mass, contains xanthones, flavonoids, tannins, and other phenolic compounds with reported antioxidant, anti-inflammatory, antimicrobial, anticancer, and antidiabetic activities (Muzykiewicz-Szymańska et al., 2020; Mahmudah et al., 2021; Gallorini et al., 2022). Among these activities, antioxidant capacity is especially important because it helps limit oxidative stress-related cellular damage associated with chronic disorders such as diabetes, cardiovascular disease, neurodegeneration, and cancer. Despite this potential, mangosteen peel is still

commonly discarded as agro-industrial waste, resulting in the loss of a valuable source of functional compounds (Chaiwarit et al., 2021). Mangosteen-derived extracts have also been explored in cosmetic and pharmaceutical-related formulations, further supporting the value of this by-product as a functional raw material rather than waste (Chaiwong et al., 2022; Sriwidodo et al., 2022). This situation has increased interest in the valorization of agricultural by-products within circular bioeconomy and sustainable food-system frameworks (Bertolo et al., 2023). In this context, green extraction technologies, especially ultrasound-assisted extraction (UAE), have attracted attention because they can improve bioactive recovery while reducing solvent consumption, extraction time, and energy demand (Pereira et al., 2025; Christou et al., 2021; Sungpud et al., 2020; Casado-Hidalgo et al., 2023; González-Silva et al., 2022). The combination of UAE with Natural Deep Eutectic Solvents (NaDES) is particularly promising because NaDES offer tunable physicochemical properties, low volatility, and good biodegradability (Airouyuwa et al., 2022; Ivanović et al., 2020; Grozdanova et al., 2020; Xu et al., 2024).

Although mangosteen peel has clear potential as a source of antioxidant compounds, its conversion into functional products still faces important challenges. Conventional extraction methods, including Soxhlet extraction, maceration, and reflux, often require toxic organic solvents, prolonged heating, and high energy input, which can reduce process efficiency and promote degradation of thermosensitive compounds (Plaza et al., 2021). Other techniques, such as optimized ultrasound-assisted extraction and related green extraction approaches, have also been applied to plant matrices, but their broader use may be limited by scale-up constraints, solvent compatibility, or cost (Demirci et al., 2022; Kobus et al., 2022; González-Silva et al., 2022). Therefore, the main research problem in this study is how to extract bioactive compounds from mangosteen peel efficiently under green-chemistry conditions while preserving antioxidant functionality. Previous studies have shown that UAE combined with ethanol or aqueous-organic solvents can improve extraction efficiency (Airouyuwa et al., 2022; Christou et al., 2021). However, many of these studies did not include standardized kinetic modeling or reproducibility-related reporting, which limits process predictability and industrial relevance (Fu et al., 2021; Tang et al., 2023).

Recent studies have highlighted NaDES as environmentally benign designer solvents whose polarity, viscosity, and hydrogen-bonding capacity can be tuned through hydrogen-bond acceptor–hydrogen-bond donor composition and water content (Pires et al., 2025; Arora et al., 2021; Yaneva et al., 2025). NaDES have also been discussed as versatile green media for isolating natural bioactive compounds from plant materials (Ivanović et al., 2020; Xu et al., 2024). Lactic acid-based, polyalcohol-based, and other NaDES systems have shown high extraction efficiency for phenolics, flavonoids, and xanthones under ultrasonic conditions (Vo et al., 2023; Mulia et al., 2019; Pavlić et al., 2022; Zhou et al., 2024). Even so, studies combining NaDES and UAE specifically for mangosteen peel remain limited. Plaza et al. (2021) used a choline chloride:glycerol NaDES system for mangosteen peel but focused mainly on yield optimization without kinetic or mechanistic analysis. In contrast, the present study applies a hybrid NaDES–VCO–EtOH system composed of choline chloride:lactose (1:2) and VCO:EtOH (1:1). This hybrid solvent was designed to reduce viscosity, broaden the cavitation window, and improve the simultaneous solubilization of hydrophilic and lipophilic antioxidants. Compared with a single-phase NaDES system, this solvent design is expected to improve acoustic energy transfer and solute

diffusion, offering a distinct approach within the UAE–NaDES framework (Pereira et al., 2025; Pires et al., 2025).

The present study also addresses several methodological gaps in the current literature. Many UAE studies on mangosteen peel still rely on single-phase ethanol/water or single NaDES systems and report only endpoint yields. In addition, ultrasound conditions are not always described in sufficient detail, particularly with respect to calibrated power delivery and clearly defined amplitude settings, which weakens reproducibility. Formal evaluation of multifactor interactions is also often limited, making it difficult to quantify the combined effects of solvent composition, temperature, and ultrasound amplitude. Finally, kinetic parameters that can connect extraction behavior, such as equilibrium yield and rate constants, with functional antioxidant outcomes are rarely incorporated into the overall interpretation. To address these limitations, this study uses a hybrid NaDES–VCO–EtOH solvent to expand solvation capacity, reports explicit UAE amplitude conditions with calorimetric calibration, applies a full 3 × 3 × 3 factorial design with three-way ANOVA including interaction terms, and integrates pseudo-second-order (PSO) kinetic modeling with DPPH radical-scavenging activity as a functional endpoint.

Beyond simple yield optimization, this work aims to connect extraction kinetics with antioxidant performance in a single analytical framework. Although antioxidant assays such as DPPH are widely used, relatively few studies have systematically linked kinetic extraction behavior to functional bioactivity. In this study, extraction performance was evaluated using three indicators: extraction yield (%) measured as the mass of dried extract recovered per initial dry mangosteen-peel mass at 60 min, antioxidant activity expressed as DPPH radical-scavenging inhibition (%), and PSO kinetic parameters, including equilibrium yield (q_e) and rate constant (k_2). Accordingly, the objectives of this study were to optimize UAE conditions for mangosteen peel extraction using a NaDES–VCO–EtOH hybrid solvent, to fit extraction kinetics using the PSO model, and to relate extraction performance to antioxidant activity through DPPH inhibition. By integrating process optimization, kinetic analysis, and functional validation, this study aims to provide a more reproducible framework for green extraction design and a clearer basis for the valorization of mangosteen peel in nutraceutical and functional-food applications.

METHOD

Research Design and Experimental Setup

This study used a full 3 × 3 × 3 factorial design to evaluate the combined effects of NaDES fraction (30, 40, and 50% v/v), temperature (30, 40, and 50 °C), and ultrasonic amplitude (60, 80, and 100%) on extraction yield and kinetic behavior. Extraction was evaluated at four time points (20, 30, 45, and 60 min) to generate kinetic profiles. Each treatment combination was performed in triplicate (n = 3), which allowed factorial ANOVA and the evaluation of interaction effects (Teixeira et al., 2023; Kobus et al., 2022; Zahari et al., 2020).

Figure 1 summarizes the overall workflow of the study, including sample preparation, UAE, post-extraction separation and drying, antioxidant assays, and kinetic and statistical analyses. This sequence was followed throughout the study to support replication and traceability.

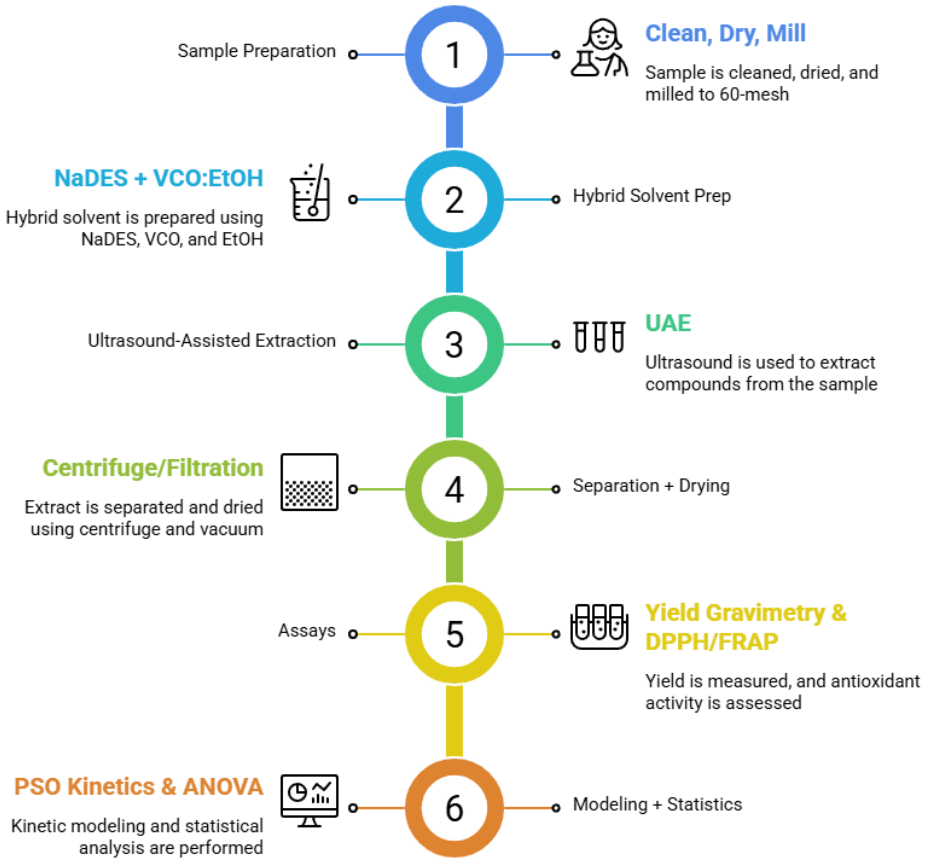

Figure 1. Workflow schematic of sample preparation, UAE, post-processing, assays, and analyses

Sample Preparation

Mangosteen (Garcinia mangostana L.) peels were cleaned, sliced, and oven-dried at 40–50 °C to limit thermal degradation of phenolic compounds during pre-treatment (Demirci et al., 2022). The dried peels were then milled and passed through a 60-mesh sieve to obtain a more uniform particle size and improve extraction contact area (González-Silva et al., 2022). The resulting powder was stored in amber glass bottles under dry conditions to minimize oxidation before extraction (Plaza et al., 2021).

NaDES Synthesis and Hybrid Solvent Preparation

NaDES was synthesized from choline chloride and lactose at a molar ratio of 1:2 by stirring the mixture at 70 ± 2 °C for 40 min until a clear and homogeneous phase formed (Alperth et al., 2024). The hybrid extraction solvent was then prepared by blending NaDES (30–50%, v/v) with virgin coconut oil (VCO) and ethanol at a VCO:EtOH ratio of 1:1 (v/v).

To support reproducibility, the physicochemical properties of each NaDES fraction were measured. Density (kg m^{-3}) was 1.123 ± 0.006 at 30%, 1.136 ± 0.004 at 40%, and 1.147 ± 0.003 at 50%. Viscosity at 40 °C (mPa·s) was 85.4 ± 1.2, 112.8 ± 1.6, and 138.6 ± 2.1, respectively. The pH measured at 25 °C was 3.86 ± 0.04, 3.73 ± 0.03, and 3.59 ± 0.02, and water activity (a_w) ranged from 0.22 to 0.28 as measured by Karl Fischer titration. These values are consistent with recent reports on choline chloride–sugar NaDES systems (Pires et al., 2025), supporting their suitability for green extraction.

Ultrasound-Assisted Extraction (UAE)

Extractions were performed using a Labtron LUHS-A10 ultrasonic processor (20 kHz, 750 W rated power) equipped with a 6 mm titanium probe. The system was operated in pulsed mode (1 s ON / 1 s OFF) to reduce thermal buildup during sonication. Each run used 2.0 g of sample and 40 mL of extraction solvent, with a probe immersion depth of approximately 2 cm. The extraction temperature was maintained at 30, 40, or 50 °C using a circulating water bath.

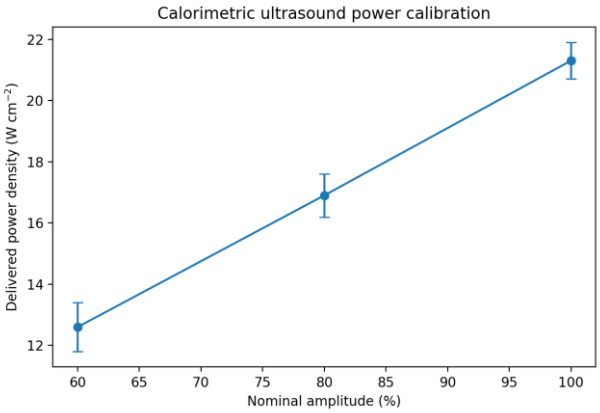

Figure 2. Calorimetric calibration of delivered acoustic power density versus nominal amplitude (mean ± SD, n = 3)

Acoustic power was calibrated by calorimetry. The delivered power densities were 12.6 ± 0.8, 16.9 ± 0.7, and 21.3 ± 0.6 W cm^{-2} at 60%, 80%, and 100% amplitude, respectively. Temperature was monitored during each run to prevent overheating, although continuous temperature time-series data were not recorded or archived. Glass vessels were cleaned between runs with ethanol and distilled water (Chuah et al., 2023). The calorimetric calibration curve is presented in Figure 2, and the temperature-monitoring procedure is summarized in Figure 3.

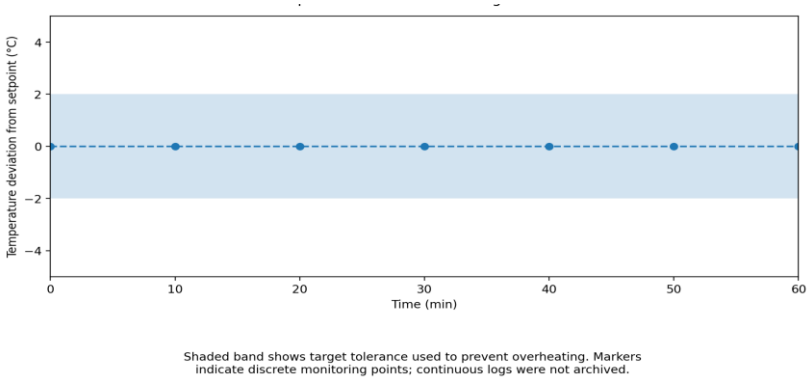

Figure 3. Temperature-control monitoring schematic used to check for overheating during UAE runs (monitoring schedule and target tolerance band). Continuous time-series temperature logs were not archived.

Extraction Yield Determination

After sonication, the extracts were centrifuged at 5000 rpm for 10 min, filtered, and vacuum-dried at 40 °C to constant mass. Extraction yield was calculated using Equation (1).

$$\text{Yield (\%)} = \frac{\text{mass of dry extract}}{\text{mass of dry sample}} \times 100 \qquad \text{(Eq. 1)}$$

Results are reported as mean ± SD (n = 3). Post-hoc comparisons of 60-min extraction yield were performed using Tukey's HSD test at α = 0.05.

Antioxidant Activity (DPPH Assay)

DPPH radical-scavenging activity was measured using the standardized stoichiometric kinetic procedure described by Angeli et al. (2021). A 0.08 mM DPPH solution in ethanol was mixed with extract solutions at concentrations of 25–200 μg mL^{-1}, incubated for 30 min in the dark at 25 °C, and then analyzed at 517 nm using a Cecil CE2021 UV–Vis spectrophotometer. Percent inhibition was calculated using Equation (2).

$$\% \text{ inhibition} = \frac{(\text{A\_blank} - \text{A\_sample})}{\text{A\_blank}} \times 100 \quad \text{(Eq. 2)}$$

All measurements were performed in triplicate (n = 3), with an acceptance criterion of CV ≤ 5%. Before each batch, the instrument baseline was set using ethanol at 517 nm. Absorbance values were blank-corrected using a DPPH reagent blank (ethanol + DPPH) and a matched extract blank (extract + ethanol without DPPH) to account for inherent sample color and turbidity. The 30-min incubation endpoint followed the standardized kinetic DPPH procedure and was verified during assay setup using representative extracts; however, full absorbance-versus-time traces were not archived for all conditions. An orthogonal FRAP assay was also conducted on selected extracts to confirm that the DPPH results were not specific to a single antioxidant assay.

Kinetic Modeling and Statistical Analysis

Extraction kinetics were analyzed using the nonlinear form of the pseudo-second-order (PSO) model and fitted by Levenberg–Marquardt optimization in OriginPro 2022 (Eq. 3).

$$Y(t) = \frac{Y_\infty^2 kt}{1 + Y_\infty kt} \quad \text{(Eq. 3)}$$

where Y(t) is the extraction yield (%) at time t, Y∞ is the equilibrium yield (%), and k_2 is the pseudo-second-order rate constant (min^{-1}). Goodness of fit was evaluated using adjusted R^2, root mean square error (RMSE), and 95% confidence intervals for both Y∞ and k_2. Residuals were also inspected for heteroscedasticity.

A three-way factorial ANOVA (NaDES × Temperature × Amplitude) was applied to the 60-min yield data to identify main effects and interaction effects, followed by Tukey's HSD post-hoc comparisons at $p < 0.05$. All statistical analyses were performed using SPSS v29 and GraphPad Prism 10. The correlation between extraction yield and DPPH activity was evaluated using Pearson's r with a 95% confidence interval. Correlations were interpreted as strong when $r > 0.7$ and significant when $p < 0.05$ (Huang et al., 2021).

RESULTS AND DISCUSSION

Extraction Yield Profiles Under Different NaDES, Temperature, and Ultrasound Amplitude Conditions

The extraction yield of *Garcinia mangostana* L. peel obtained with the hybrid NaDES–VCO–EtOH solvent under ultrasound-assisted extraction (UAE) depended on extraction time, NaDES concentration, temperature, and ultrasound amplitude.

Yield values from the 27 treatment combinations (n = 3) are presented in Tables 1–3 for 30%, 40%, and 50% NaDES, respectively.

Table 1. Extraction Yield (%) at 30% NaDES (VCO:EtOH = 1:1)

Amplitude (%)	Temperature (°C)	20 min	30 min	45 min	60 min
60	30	12.1 ± 0.2^{a}	12.6 ± 0.2^{a}	13.0 ± 0.2^{a}	13.2 ± 0.3^{a}
80	30	13.4 ± 0.3^{ab}	13.9 ± 0.3^{b}	14.3 ± 0.3^{b}	14.7 ± 0.3^{b}
100	30	14.8 ± 0.3^{c}	15.3 ± 0.3^{c}	15.7 ± 0.3^{c}	16.1 ± 0.4^{c}
60	40	13.0 ± 0.2^{a}	13.5 ± 0.3^{a}	14.0 ± 0.3^{a}	14.4 ± 0.3^{a}
80	40	14.8 ± 0.3^{b}	15.3 ± 0.3^{b}	15.8 ± 0.3^{b}	16.2 ± 0.4^{b}
100	40	16.2 ± 0.3^{c}	16.8 ± 0.3^{c}	17.3 ± 0.3^{c}	17.9 ± 0.4^{c}
60	50	14.0 ± 0.3^{a}	14.6 ± 0.3^{a}	15.2 ± 0.3^{a}	15.7 ± 0.3^{a}
80	50	16.5 ± 0.3^{b}	17.1 ± 0.3^{b}	17.6 ± 0.3^{b}	18.1 ± 0.4^{b}
100	50	20.5 ± 0.4^{c}	21.1 ± 0.4^{c}	21.6 ± 0.4^{c}	22.2 ± 0.4^{c}

All values are reported as mean ± SD. Different superscript letters indicate significant differences within each temperature row based on Tukey's HSD post-hoc comparison (α = 0.05), which is presented here as a descriptive simple-effect comparison among amplitudes at fixed NaDES concentration and time point. Main effects and interaction effects were evaluated separately using the three-way ANOVA summary shown in Table 4.

Table 2. Extraction Yield (%) at 40% NaDES (VCO:EtOH = 1:1)

Amplitude (%)	Temperature (°C)	20 min	30 min	45 min	60 min
60	30	13.8 ± 0.3^{a}	14.4 ± 0.3^{a}	14.9 ± 0.3^{a}	15.4 ± 0.3^{a}
80	30	15.6 ± 0.3^{b}	16.2 ± 0.3^{b}	16.8 ± 0.3^{b}	17.4 ± 0.3^{b}
100	30	17.6 ± 0.3^{c}	18.3 ± 0.3^{c}	18.9 ± 0.3^{c}	19.5 ± 0.3^{c}
60	40	14.7 ± 0.3^{a}	15.4 ± 0.3^{a}	16.0 ± 0.3^{a}	16.6 ± 0.3^{a}
80	40	16.8 ± 0.3^{b}	17.4 ± 0.3^{b}	18.0 ± 0.3^{b}	20.3 ± 0.4^{b}
100	40	18.3 ± 0.3^{c}	19.0 ± 0.3^{c}	19.6 ± 0.4^{c}	22.0 ± 0.4^{c}
60	50	15.9 ± 0.3^{a}	16.6 ± 0.3^{a}	17.2 ± 0.3^{a}	17.8 ± 0.3^{a}
80	50	18.1 ± 0.3^{b}	18.8 ± 0.3^{b}	19.4 ± 0.3^{b}	20.1 ± 0.3^{b}
100	50	22.4 ± 0.4^{c}	23.2 ± 0.4^{c}	23.9 ± 0.4^{c}	25.1 ± 0.4^{c}

Across all solvent compositions, extraction yield increased with time, with the largest increase occurring between 20 and 45 min. The yield then approached a plateau between 45 and 60 min, indicating that most solute transfer occurred during the earlier phase of extraction. At 30% NaDES, the 60-min yield ranged from 13.2 ± 0.3% to 22.2 ± 0.4% depending on temperature and amplitude (Table 1). At 40% NaDES, the corresponding range increased to 15.4 ± 0.3%–25.1 ± 0.4% (Table 2). At 50% NaDES, the 60-min yield ranged from 16.8 ± 0.3% to 26.2 ± 0.4% (Table 3). The highest measured yield was obtained at 50% NaDES, 50 °C, and 100% amplitude.

Table 3. Extraction Yield (%) at 50% NaDES (VCO:EtOH = 1:1)

Amplitude (%)	Temperature (°C)	20 min	30 min	45 min	60 min
60	30	14.9 ± 0.3^{a}	15.6 ± 0.3^{a}	16.2 ± 0.3^{a}	16.8 ± 0.3^{a}
80	30	17.0 ± 0.3^{b}	17.7 ± 0.3^{b}	18.3 ± 0.3^{b}	18.9 ± 0.3^{b}
100	30	19.2 ± 0.3^{c}	20.0 ± 0.3^{c}	20.7 ± 0.4^{c}	21.5 ± 0.4^{c}
60	40	16.1 ± 0.3^{a}	16.8 ± 0.3^{a}	17.5 ± 0.3^{a}	18.2 ± 0.3^{a}
80	40	18.5 ± 0.3^{b}	19.3 ± 0.3^{b}	20.0 ± 0.3^{b}	20.7 ± 0.3^{b}
100	40	21.0 ± 0.3^{c}	21.8 ± 0.4^{c}	22.5 ± 0.4^{c}	23.4 ± 0.4^{c}

Amplitude (%)	Temperature (°C)	20 min	30 min	45 min	60 min
60	50	17.2 ± 0.3[a]	18.0 ± 0.3[a]	18.7 ± 0.3[a]	19.4 ± 0.3[a]
80	50	20.0 ± 0.3[b]	20.7 ± 0.3[b]	21.5 ± 0.3[b]	22.2 ± 0.3[b]
100	50	24.9 ± 0.4[c]	25.5 ± 0.4[c]	25.8 ± 0.4[c]	26.2 ± 0.4[c]

Three-way ANOVA of the 60-min yields confirmed significant main effects of NaDES concentration, temperature, and amplitude ($p < 0.001$), together with significant two-way and three-way interactions (Table 4). Amplitude showed the largest effect size (partial $\eta^2 = 0.983$), followed by NaDES concentration (partial $\eta^2 = 0.976$) and temperature (partial $\eta^2 = 0.967$). Among the interaction terms, Temperature × Amplitude showed the strongest interaction effect (partial $\eta^2 = 0.803$), indicating that the influence of amplitude varied with temperature. This interaction pattern is illustrated in Figure 4.

Table 4. Three-way factorial ANOVA summary for 60-min extraction yield (n = 3 per cell)

Source	df	SS	MS	F	p	partial η^2
NaDES	2	259.727	129.863	1095.7	<0.001	0.976
Temperature	2	184.860	92.430	779.9	<0.001	0.967
Amplitude	2	359.807	179.903	1517.9	<0.001	0.983
NaDES × Temperature	4	3.133	0.783	6.6	<0.001	0.329
NaDES × Amplitude	4	5.047	1.262	10.6	<0.001	0.441
Temperature × Amplitude	4	26.093	6.523	55.0	<0.001	0.803
NaDES × Temperature × Amplitude	8	3.333	0.417	3.5	0.002	0.342
Error	54	6.400	0.119			
Total	**80**	**848.400**				

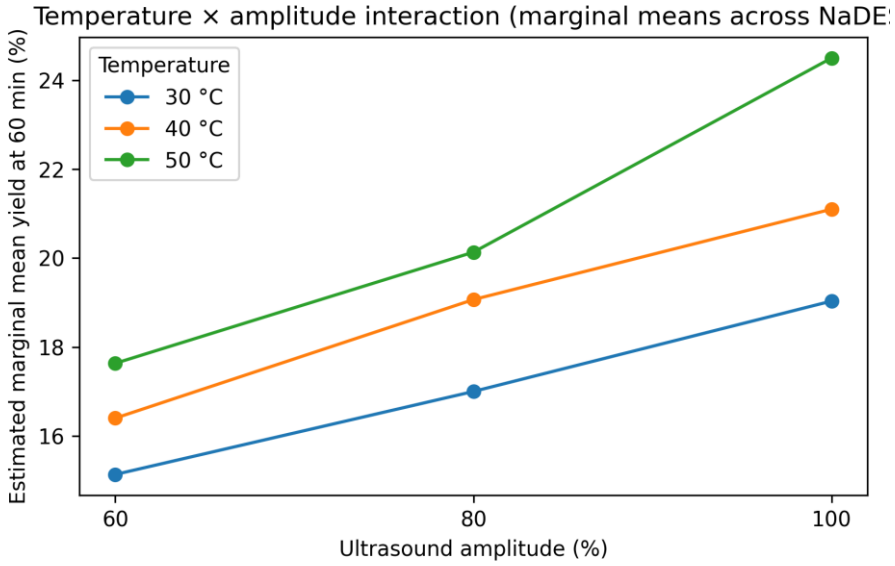

Figure 4. Temperature × amplitude interaction plot (estimated marginal means for 60-min extraction yield, averaged across NaDES levels; n = 3 per cell).

Pseudo-Second-Order (PSO) Kinetic Modeling of Extraction Yield

The pseudo-second-order (PSO) kinetic model was used to evaluate the extraction dynamics of the NaDES–VCO–EtOH system under UAE. The nonlinear form applied in this study was $Y(t) = (Y\infty^2 kt) / (1 + Y\infty kt)$, where Y(t) is the extraction

yield (%) at time t, Y_∞ is the equilibrium yield (%), k_2 is the pseudo-second-order rate constant (min^{-1}), and t is the extraction time (min).

Table 5. PSO Kinetic Parameters per Treatment

NaDES (%)	Temp (°C)	Amplitude (%)	k_2 (min^{-1})	q_e (%)	RMSE
30	30	60	0.0252	13.83	0.0108
	30	80	0.0221	15.33	0.0711
	30	100	0.0225	16.72	0.0721
	40	60	0.0197	15.11	0.0770
	40	80	0.0202	16.89	0.0787
	40	100	0.0169	18.68	0.1247
	50	60	0.0158	16.58	0.0964
	50	80	0.0179	18.87	0.0928
	50	100	0.0176	22.94	0.1275
40	30	60	0.0173	16.20	0.0904
	30	80	0.0154	18.27	0.1285
	30	100	0.0148	20.43	0.1129
	40	60	0.0142	17.56	0.1097
	40	80	0.0075	21.48	0.6684
	40	100	0.0072	23.24	0.6884
	50	60	0.0144	18.75	0.1111
	50	80	0.0142	21.03	0.1452
	50	100	0.0107	26.19	0.2964
50	30	60	0.0142	17.76	0.1099
	30	80	0.0147	19.83	0.1123
	30	100	0.0121	22.59	0.1649
	40	60	0.0128	19.24	0.1474
	40	80	0.0125	21.79	0.1324
	40	100	0.0118	24.48	0.1987
	50	60	0.0123	20.51	0.1309
	50	80	0.0126	23.27	0.1598
	50	100	0.0245	26.78	0.0670

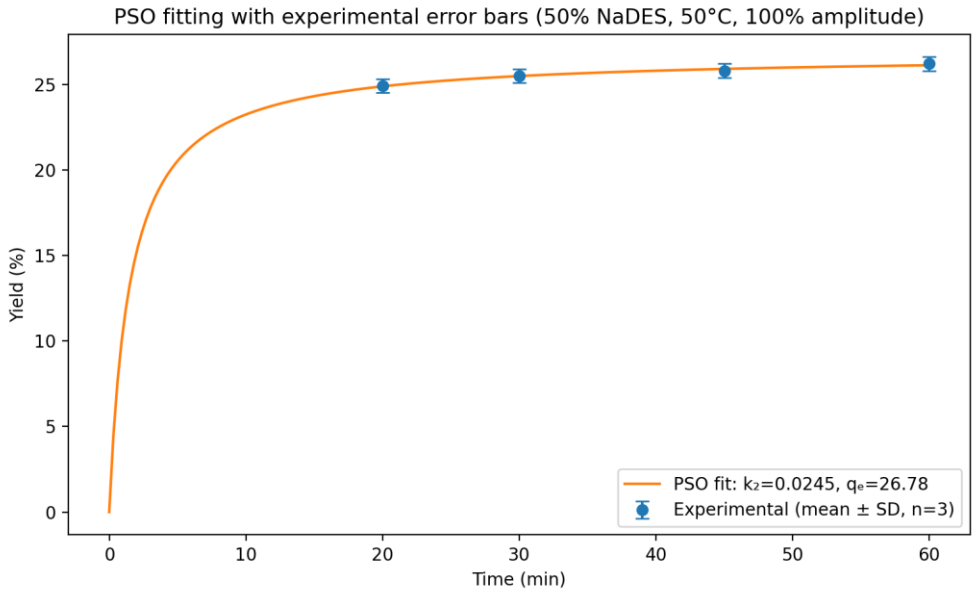

Figure 5. PSO model fit versus experimental yield (mean ± SD, n = 3) with error bars. NaDES = 50%, Temp = 50 °C, Amp = 100%.

The model was fitted by Levenberg–Marquardt optimization in OriginPro 2022 using yield data collected at 20, 30, 45, and 60 min for all 27 treatment combinations. Table 5 summarizes the estimated k_2, q_e, and RMSE values. Across all treatments, the model described the overall extraction trajectories with RMSE values ranging from 0.011 to 0.688. Most treatments showed low deviation from the fitted curve, whereas two treatments at 40% NaDES and 40 °C under 80% and 100% amplitude showed larger RMSE values (approximately 0.67–0.69).

The highest equilibrium yield was obtained at 50% NaDES, 50 °C, and 100% amplitude, where q_e reached 26.78%. The next highest q_e value was observed at 40% NaDES, 50 °C, and 100% amplitude (26.19%). These values were consistent with the experimental pattern observed in previous section (Extraction Yield Profiles Under Different NaDES, Temperature, and Ultrasound Amplitude Conditions), in which higher NaDES concentration, higher temperature, and higher amplitude generally increased the extraction yield. Figures 5 and 6 show representative PSO fits for the two best-performing conditions. In both cases, the fitted curves followed the experimental mean values closely, indicating that the model adequately represented the extraction profile under these conditions.

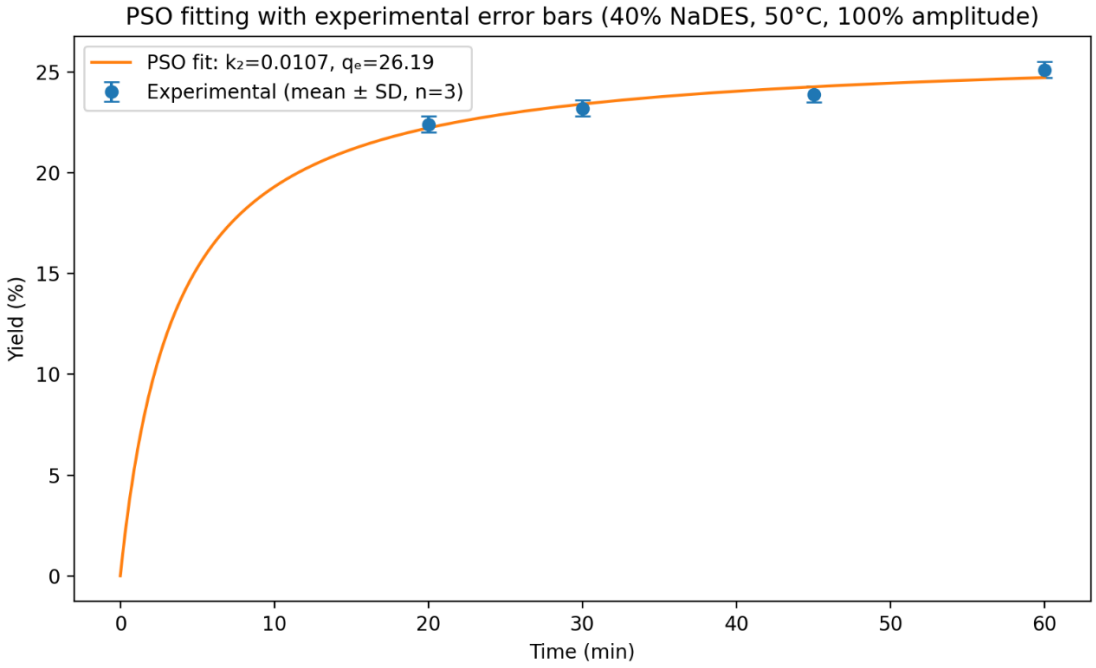

Figure 6. PSO model fit versus experimental yield (mean ± SD, n = 3) with error bars. NaDES = 40%, Temp = 50 °C, Amp = 100%

Antioxidant Activity and Its Correlation with Extraction Yield

The antioxidant activity of the mangosteen peel extracts was evaluated using the DPPH radical-scavenging assay. The 60-min extracts were analyzed because this time point corresponded to the plateau region identified from the PSO profiles (see section: Pseudo-Second-Order (PSO) Kinetic Modeling of Extraction Yield). Table 6 presents DPPH inhibition together with extraction yield for representative conditions. The highest antioxidant activity was recorded at 50% NaDES, 50 °C, and 100% amplitude, where DPPH inhibition reached 94.4 ± 0.8% and the measured extraction yield reached 26.2 ± 0.5%. The lowest DPPH inhibition was observed at 30% NaDES, 30 °C, and 60% amplitude, where inhibition was 57.4 ± 1.6%.

A Pearson correlation analysis showed a strong positive relationship between extraction yield and DPPH inhibition ($r = 0.88$, 95% CI = 0.79–0.93, $p < 0.01$), as shown in Figure 7. The FRAP assay performed on representative low-, medium-, and high-intensity extracts showed the same ranking pattern as the DPPH assay. The extract obtained at 50% NaDES, 50 °C, and 100% amplitude had the highest FRAP value (879.5 ± 15.6 µmol Fe^{2+}/g extract), followed by 40–50–100 (755.2 ± 13.4 µmol Fe^{2+}/g) and 30–30–60 (389.8 ± 10.5 µmol Fe^{2+}/g). The linear association between DPPH and FRAP was also positive ($r = 0.86$, $p < 0.01$), supporting agreement between the two antioxidant assays.

Table 6. DPPH Inhibition and Extraction Yield at 60 Minutes (mean ± SD, n = 3)

NaDES (%)	Temp (°C)	Amp (%)	Yield (%)	DPPH Inhibition (%)
30	30	60	13.2 ± 0.4[a]	57.4 ± 1.6[a]
30	30	80	14.7 ± 0.5[ab]	62.6 ± 1.8[b]
30	30	100	16.1 ± 0.5[b]	67.0 ± 1.5[c]
30	40	60	14.4 ± 0.3[a]	59.1 ± 1.4[a]
30	40	80	16.2 ± 0.4[b]	64.5 ± 1.6[b]
30	40	100	17.9 ± 0.6[c]	69.6 ± 1.7[c]
30	50	60	15.7 ± 0.3[b]	64.0 ± 1.3[b]
30	50	80	18.1 ± 0.4[c]	69.4 ± 1.4[c]
30	50	100	22.2 ± 0.5[d]	83.4 ± 1.2[e]
40	50	100	25.1 ± 0.6[e]	89.1 ± 1.0[f]
50	50	100	26.2 ± 0.5[e]	94.4 ± 0.8[g]

[a–g] Different superscript letters indicate significant differences ($p < 0.05$, Tukey's HSD).

Factorial inference is presented for the 60-min extraction yield via three-way ANOVA (Table 4). For antioxidant endpoints (DPPH; and FRAP where reported), the results are presented as functional validation using mean ± SD and correlation patterns rather than full-factorial post-hoc inference.

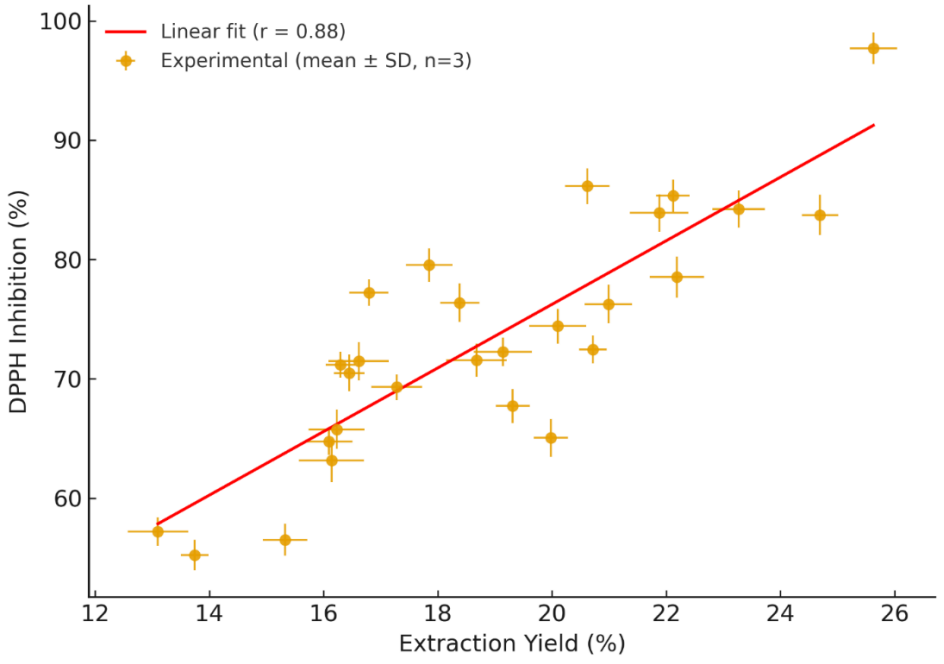

Figure 7. Correlation between Extraction Yield (%) and DPPH Inhibition (%) for all UAE conditions at 60 min (mean ± SD, n = 3, $r = 0.88$, $p < 0.01$).

Discussion

Effects of NaDES Concentration, Temperature, and Ultrasound Amplitude on Extraction Performance

The results show that extraction performance improved as NaDES concentration, temperature, and amplitude increased within the studied range. The steady rise in yield from 20 to 45 min, followed by a plateau between 45 and 60 min, indicates that the extraction process was initially governed by rapid solute transfer and later approached equilibrium. The strong main effects identified by ANOVA, together with the significant interaction terms, indicate that the three factors did not act independently. In particular, the strong Temperature × Amplitude interaction suggests that the effect of higher ultrasound intensity depended on the thermal condition of the extraction system. This pattern is consistent with previous reports showing that NaDES-assisted extraction and UAE can improve polyphenol and flavonoid recovery by enhancing solvent–solute interactions and mass transfer in plant matrices (Pavlić et al., 2022; Zhou et al., 2024). More broadly, the relevance of solvent choice in green extraction has also been highlighted in comparisons between classical green solvents and NaDES systems (Yaneva et al., 2025).

The improvement observed at higher NaDES levels can be attributed to enhanced solvent–solute interactions and improved solubilization of target compounds, whereas the effect of temperature likely reflects reduced viscosity and improved diffusivity. The contribution of amplitude is consistent with increased cavitation intensity and stronger disruption of plant tissues. Taken together, these patterns support the interpretation that solvent composition and ultrasound conditions acted synergistically to improve mass transfer under the hybrid NaDES–VCO–EtOH system.

Interpretation of PSO Kinetic Behavior

The PSO model adequately described most extraction profiles and provided a useful estimate of equilibrium yield across the 27 treatment combinations. The highest q_e value at 50% NaDES, 50 °C, and 100% amplitude agreed closely with the experimentally measured optimum, indicating that the model captured the dominant extraction behavior under the best-performing condition. This result is consistent with earlier reports that PSO kinetics can describe extraction systems influenced by both external mass transfer and internal diffusion processes (Zahari et al., 2020; Liang et al., 2020).

Although higher temperature and amplitude generally increased q_e, their effects on k_2 were not fully linear. The reduced k_2 values under some high-intensity conditions, especially at 40% NaDES and 40 °C, may indicate transient deviations from the ideal PSO assumption. Such deviations may arise from changes in local viscosity, variable cavitation behavior, or measurement variability at later extraction times. Similar nonlinear behavior under ultrasound-assisted NaDES extraction has been discussed in previous studies (Lanjekar & Rathod, 2021; Shikov et al., 2022). The close agreement between the fitted curves and the experimental data in Figures 3 and 4 therefore supports the use of PSO as a practical model for process interpretation, while also indicating that some treatment combinations may require more flexible kinetic descriptions in future studies.

Functional Implications of the Yield–Antioxidant Relationship

The strong positive correlation between extraction yield and DPPH inhibition indicates that conditions favoring higher solute recovery also favored recovery of antioxidant-active compounds. This pattern is consistent with the known abundance of polyphenols and xanthones in mangosteen peel and with the capacity of hybrid solvent systems to recover compounds with different polarity characteristics (Mahmudah et al., 2021; John et al., 2022; González-Laredo et al., 2023; Kiene et al., 2024). It is also in line with studies showing a close relationship between extraction efficiency and antioxidant response in plant extracts (Yang & Li, 2022). The FRAP results further strengthened this interpretation because the ranking of extracts remained consistent across both assays. The agreement between DPPH and FRAP suggests that the observed antioxidant trend was not an artifact of a single analytical method.

The combined results from yield, PSO modeling, DPPH, and FRAP indicate that the optimum condition of 50% NaDES, 50 °C, and 100% amplitude produced the most favorable balance between extraction performance and functional antioxidant recovery in the investigated design space. These findings support the value of integrating kinetic analysis with antioxidant evaluation when optimizing green extraction systems for mangosteen peel. Such integration can strengthen process interpretation and provide a clearer basis for future scale-up and nutraceutical applications (Mahmudah et al., 2021; Hao et al., 2020; Rizaldy et al., 2022).

CONCLUSION

This study demonstrates that integrating ultrasound-assisted extraction (UAE) with a NaDES–VCO–EtOH hybrid solvent system provides an effective and sustainable approach for enhancing the recovery and antioxidant performance of compounds extracted from Garcinia mangostana L. peel. Using a full 3 × 3 × 3 factorial design and pseudo-second-order (PSO) kinetic modeling, the study identified the effects of NaDES concentration, temperature, and ultrasound amplitude on extraction behavior within the investigated operating range. Extraction yield and antioxidant activity were strongly correlated ($r = 0.88$, 95% CI: 0.79–0.93, $p < 0.01$), indicating that conditions favoring higher solute recovery also favored stronger antioxidant responses. Rather than confirming exact physicochemical mechanisms, these findings support the interpretation that cavitation-enhanced mass transfer, solvent–solute affinity, and viscosity-related diffusional effects jointly contributed to extraction performance under the studied conditions.

Under the optimum condition of 50% NaDES, 50 °C, 100% amplitude, and 60 min extraction time, the process produced an extraction yield of 26.2 ± 0.5%, DPPH inhibition of 94.4 ± 0.8%, FRAP activity of 879.5 ± 15.6 μmol Fe^{2+} g^{-1} extract, and PSO kinetic parameters of $k_2 = 0.0245$ min^{-1}, $q_e = 26.78\%$, and RMSE = 0.067. The viscosity also decreased from 43.6 to 28.1 mPa·s at 40–50 °C for 50% NaDES, which is consistent with improved mass-transfer conditions. Among the tested variables, amplitude was the most influential factor (partial $\eta^2 = 0.983$; $p < 0.001$; Table 4), followed by NaDES concentration and temperature. The agreement between DPPH and FRAP results further supports the reliability of the antioxidant evaluation. Overall, the hybrid UAE–NaDES–VCO–EtOH system achieved high extraction yield and strong antioxidant activity within the studied design space, while the PSO model adequately described the extraction dynamics under most treatment conditions.

RECOMMENDATION

For laboratory-scale and pilot-scale application, the results support the use of 50% NaDES (ChCl : Lactose = 1 : 2 mol/mol), 50 °C, 100% amplitude, and 60 min as the most favorable operating condition within the tested range. Process control should include pulsed sonication (1 s ON / 1 s OFF), consistent probe immersion depth, and solvent temperatures maintained at or below 50 °C to reduce thermal buildup and limit degradation of heat-sensitive constituents. Preheating the NaDES phase to approximately 45 °C may also help reduce viscosity and improve cavitation efficiency. Within the validated operating domain, PSO parameters such as k_2 and q_e, together with RMSE, may serve as useful indicators for monitoring extraction performance.

For scale-up development, future process design should evaluate continuous-flow sonochemical reactors and in-line viscosity monitoring to improve process stability and mass-transfer reproducibility at larger scale. Controlled solvent-reuse studies are also needed and should report per-cycle yield, antioxidant responses, and solvent stability indicators such as viscosity, water content, and FTIR/NMR fingerprints. In addition, direct benchmarking against an ethanol-only extraction conducted under identical UAE conditions, including the same solid–liquid ratio, extraction time, temperature, and calorimetrically calibrated delivered power, is required before making head-to-head performance claims.

Future research should also strengthen mechanistic and applied understanding by using response surface modeling (RSM) or generalized linear modeling (GLM) to map multifactor interactions with greater resolution, by including orthogonal antioxidant assays such as ABTS or ORAC, and by applying targeted metabolomic profiling to relate xanthones and phenolics to kinetic behavior more specifically. Further work should incorporate life-cycle assessment (LCA), energy–cost modeling, and explicit green metrics such as E-factor and specific energy input with clearly defined system boundaries, solvent recovery assumptions, and treatment of mass and energy losses. Additional studies should also include continuous temperature logging during representative runs and explore alternative NaDES formulations, including ChCl–lactic acid and ChCl–proline systems, to evaluate how solvent composition influences polarity, recyclability, and extraction performance.

Acknowledgment

The authors would like to express their sincere gratitude to the Directorate of Research and Community Service, Directorate General of Research and Development, Ministry of Higher Education, Science, and Technology of Indonesia, for providing financial support through the Budget Implementation List, Fiscal Year 2025. In addition, the authors gratefully acknowledge the administrative assistance provided by their home institutions, as well as the technical support received during laboratory work. The authors also extend their appreciation to the Chemistry Laboratory, Department of Chemistry, Faculty of Mathematics and Natural Sciences, Tadulako University, for providing materials and facilities that greatly contributed to the success of this research.

Funding Information

This research was funded by the Budget Implementation List of the Directorate of Research and Community Service, Directorate General of Research and Development, Ministry of Higher Education, Science, and Technology Indonesia, Fiscal Year 2025, grant number 114/C3/DT.05.00/PL/2025, dated 28 May 2025. The same institution funded the APC.

Conflict of Interest Statement

Authors state no conflict of interest.

Data Availability

Data availability is not applicable to this article because no new data were created or analyzed in this study.

Ethical Statement

Not Applicable.

Author Contributions Statement

Name of Author	C	M	So	Va	Fo	I	R	D	O	E	Vi	Su	P	Fu
Jusman	✓	✓							✓					
Moh. Mirzan	✓									✓				
Ahmad Ridhay			✓		✓	✓					✓			
Citra Risty Andini		✓	✓			✓								
Novrita A. Sangkala		✓					✓						✓	
Siti Nur Aisyah	✓											✓		✓

C : **C**onceptualization
M : **M**ethodology
So : **So**ftware
Va : **Va**lidation
Fo : **Fo**rmal analysis
I : **I**nvestigation
R : **R**esources
D : **D**ata Curation
O : Writing - **O**riginal Draft
E : Writing - Review & **E**diting
Vi : **Vi**sualization
Su : **Su**pervision
P : **P**roject administration
Fu : **Fu**nding acquisition

REFERENCES

Airouyuwa, J., Mostafa, H., Riaz, A., & Maqsood, S. (2022). Utilization of natural deep eutectic solvents and ultrasound-assisted extraction as a green extraction technique for the recovery of bioactive compounds from date palm (Phoenix dactylifera L.) seeds: An investigation into optimization of process parameters. *Ultrasonics Sonochemistry, 91*, 106233. https://doi.org/10.1016/j.ultsonch.2022.106233

Alperth, F., Feistritzer, T., Huber, M., Kunert, O., & Bučar, F. (2024). Natural deep eutectic solvents for the extraction of spilanthol from Acmella oleracea (L.) R.K.Jansen. *Molecules, 29*(3), 612. https://doi.org/10.3390/molecules29030612

Angeli, L., Imperiale, S., Ding, Y., Scampicchio, M., & Morozova, K. (2021). A novel stoichio-kinetic model for the DPPH assay: The importance of the side reaction and application to complex mixtures. *Antioxidants, 10*(7), 1019. https://doi.org/10.3390/antiox10071019

Arora, S., Gupta, N., & Singh, V. (2021). pH-controlled efficient conversion of hemicellulose to furfural using choline-based deep eutectic solvents as catalysts. *ChemSusChem, 14*(18), 3953–3958. https://doi.org/10.1002/cssc.202101130

Bertolo, M., Bogusz, S., & Mitchell, A. (2023). Green strategies for recovery of bioactive phenolic compounds from agro-industrial wastes (pomegranate peels, almond hulls, and elderberry pomace) using natural deep eutectic solvents. *ACS Food Science & Technology, 3*(12), 2144–2156. https://doi.org/10.1021/acsfoodscitech.3c00367

Casado-Hidalgo, G., Morante-Zarcero, S., Pérez-Quintanilla, D., & Sierra, I. (2023). Design and optimisation of sustainable sample treatments based on ultrasound-assisted extraction and strong cation-exchange purification with functionalised SBA-15 for opium alkaloids in ground poppy seeds. *Toxins, 15*(12), 672. https://doi.org/10.3390/toxins15120672

Chaiwarit, T., Kantrong, N., Sommano, S., Rachtanapun, P., Junmahasathien, T., Kumpugdee-Vollrath, M., & Jantrawut, P. (2021). Extraction of tropical fruit

peels and development of HPMC film containing the extracts as an active antibacterial packaging material. *Molecules, 26*(8), 2265. https://doi.org/10.3390/molecules26082265

Chaiwong, N., Phimolsiripol, Y., Leelapornpisid, P., Ruksiriwanich, W., Jantanasakulwong, K., Rachtanapun, P., & Punyodom, W. (2022). Synergistic effects of carboxymethyl chitosan and mangosteen extract on enhancing moisturizing, antioxidant, antibacterial, and deodorizing properties in emulsion cream. *Polymers, 14*(1), 178. https://doi.org/10.3390/polym14010178

Christou, A., Stavrou, I., & Kapnissi-Christodoulou, C. (2021). Continuous and pulsed ultrasound-assisted extraction of carob's antioxidants: Processing parameters optimization and identification of polyphenolic composition. *Ultrasonics Sonochemistry, 76*, 105630. https://doi.org/10.1016/j.ultsonch.2021.105630

Chuah, W., Lee, H., Ng, D., Ho, A., Sulaiman, M., & Chye, F. (2023). Discovery of antioxidants for the differentiation of monofloral stingless bee honeys using ambient mass spectrometry and metabolomics approaches. *Foods, 12*(12), 2404. https://doi.org/10.3390/foods12122404

Demirci, M., Tomaş, M., Tekin-Cakmak, Z., & Karasu, S. (2022). *Berberis crataegina DC.* as a novel natural food colorant source: Ultrasound-assisted extraction optimization using response surface methodology and thermal stability studies. *Food Science and Technology, 42*. https://doi.org/10.1590/fst.13421

Fu, X., Wang, D., Belwal, T., Xu, Y., Li, L., & Luo, Z. (2021). Sonication-synergistic natural deep eutectic solvent as a green and efficient approach for extraction of phenolic compounds from peels of *Carya cathayensis* Sarg. *Food Chemistry, 355*, 129577. https://doi.org/10.1016/j.foodchem.2021.129577

Gallorini, M., Carradori, S., Resende, D., Saso, L., Ricci, A., Palmeira, A., & Sousa, E. (2022). Natural and synthetic xanthone derivatives counteract oxidative stress via Nrf2 modulation in inflamed human macrophages. *International Journal of Molecular Sciences, 23*(21), 13319. https://doi.org/10.3390/ijms232113319

González-Laredo, R., Sayago-Monreal, V., Moreno-Jiménez, M., Rocha-Guzmán, N., Gallegos-Infante, J., Landeros-Macías, L., Y Rosales-Castro, M. (2023). Natural deep eutectic solvents (NaDES) as an emerging technology for the valorisation of natural products and agro-food residues: A review. *International Journal of Food Science & Technology, 58*(12), 6660–6673. https://doi.org/10.1111/ijfs.16641

González-Silva, N., Nolasco-González, Y., Aguilar-Hernández, G., Sáyago-Ayerdi, S., Villagrán, Z., Acosta, J., & Anaya-Esparza, L. (2022). Ultrasound-assisted extraction of phenolic compounds from *Psidium cattleianum* leaves: Optimization using the response surface methodology. *Molecules, 27*(11), 3557. https://doi.org/10.3390/molecules27113557

Grozdanova, T., Trusheva, B., Alipieva, K., Popova, M., Dimitrova, L., Najdenski, H., & Bankova, V. (2020). Extracts of medicinal plants with natural deep eutectic solvents: Enhanced antimicrobial activity and low genotoxicity. *BMC Chemistry, 14*(1), 1–9. https://doi.org/10.1186/s13065-020-00726-x

Hao, C., Chen, L., Dong, H., Xing, W., Xue, F., & Cheng, Y. (2020). Extraction of flavonoids from *Scutellariae radix* using ultrasound-assisted deep eutectic solvents and evaluation of their anti-inflammatory activities. *ACS Omega, 5*(36), 23140–23147. https://doi.org/10.1021/acsomega.0c02898

Huang, X., Zhou, X., Dai, Q., & Qin, Z. (2021). Antibacterial, antioxidation, UV-blocking, and biodegradable soy protein isolate food packaging film with

mangosteen peel extract and ZnO nanoparticles. *Nanomaterials, 11*(12), 3337. https://doi.org/10.3390/nano11123337

Ivanović, M., Razboršek, M., & Kolar, M. (2020). Innovative extraction techniques using deep eutectic solvents and analytical methods for the isolation and characterization of natural bioactive compounds from plant material. *Plants, 9*(11), 1428. https://doi.org/10.3390/plants9111428

John, O., Mushunje, A., Surugau, N., & Guad, R. (2022). The metabolic and molecular mechanisms of α-mangostin in cardiometabolic disorders (Review). *International Journal of Molecular Medicine, 50*(3). https://doi.org/10.3892/ijmm.2022.5176

Kiene, M., Zaremba, M., Januschewski, E., Juadjur, A., Jerz, G., & Winterhalter, P. (2024). Sustainable in silico-supported ultrasonic-assisted extraction of oligomeric stilbenoids from grapevine roots using natural deep eutectic solvents (NaDES) and stability study of potential ready-to-use extracts. *Foods, 13*(2), 324. https://doi.org/10.3390/foods13020324

Kobus, Z., Pecyna, A., Buczaj, A., Krzywicka, M., Przywara, A., & Nadulski, R. (2022). Optimization of the ultrasound-assisted extraction of bioactive compounds from *Cannabis sativa* L. leaves and inflorescences using response surface methodology. *Applied Sciences, 12*(13), 6747. https://doi.org/10.3390/app12136747

Lanjekar, K., & Rathod, V. (2021). Application of ultrasound and natural deep eutectic solvent for the extraction of glycyrrhizic acid from *Glycyrrhiza glabra*: Optimization and kinetic evaluation. *Industrial & Engineering Chemistry Research, 60*(26), 9532–9538. https://doi.org/10.1021/acs.iecr.1c00862

Liang, X., Hu, Y., Li, J., Chang, A., Xia, T., Li, Y., & Jiang, Z. (2020). Identification and pharmacokinetics of quinone reductase two inhibitors after oral administration of *Garcinia mangostana* L. extract in rats by LC–MS/MS. *Journal of Agricultural and Food Chemistry, 68*(43), 11975–11986. https://doi.org/10.1021/acs.jafc.0c04439

Mahmudah, R., Adnyana, I., & Sukandar, E. (2021). Molecular docking studies of α-mangostin, γ-mangostin, and xanthone on peroxisome proliferator-activated receptor gamma, diphenyl peptidase-4 enzyme, and aldose reductase enzyme as an antidiabetic drug candidate. *Journal of Advanced Pharmaceutical Technology & Research, 12*(2), 196–208. https://doi.org/10.4103/japtr.japtr_255_20

Mulia, K., Fauzia, F., & Krisant, E. A. (2019). Polyalcohols as hydrogen-bonding donors in choline chloride-based deep eutectic solvents for extraction of xanthones from the pericarp of *Garcinia mangostana* L. *Molecules, 24*(3), 636. https://doi.org/10.3390/molecules24030636

Muzykiewicz-Szymańska, A., Zielonka-Brzezicka, J., Siemak, J., & Klimowicz, A. (2020). Antioxidant activity and polyphenol content in extracts from various parts of fresh and frozen mangosteen. *Acta Scientiarum Polonorum Technologia Alimentaria, 19*(3), 261–270. https://doi.org/10.17306/j.afs.0788

Pavlić, B., Mrkonjić, Ž., Teslić, N., Cvetanović, A., Pojić, M., Mandić, A., & Mišan, A. (2022). Natural deep eutectic solvent (NaDES) extraction improves polyphenol yield and antioxidant activity of wild thyme (*Thymus serpyllum* L.) extracts. *Molecules, 27*(5), 1508. https://doi.org/10.3390/molecules27051508

Pereira, T. C., Souza, V. P., Padilha, A. P. F., Duarte, F. A., & Flores, E. M. M. (2025). Trends and perspectives on the ultrasound-assisted extraction of bioactive compounds using natural deep eutectic solvents. *Current Opinion in Chemical Engineering, 47*, 101088. https://doi.org/10.1016/j.coche.2024.101088

Pires, I. V., Rodrigues, A. M. da C., Pinheiro, W. B. de S., Cardoso, L. N., Filho, C., Saldaña, M. D. A., & da Silva, L. H. M. (2025). Physicochemical properties, antioxidant potential, and spectroscopic investigation of choline chloride–lactic acid NaDES: Effects of molar ratio and added water. Journal of Molecular Liquids, 437(Part B), 128414. https://doi.org/10.1016/j.molliq.2025.128414

Plaza, M., Domínguez-Rodríguez, G., Sahelices, C., & Marina, M. (2021). A sustainable approach for extracting non-extractable phenolic compounds from mangosteen peel using ultrasound-assisted extraction and natural deep eutectic solvents. *Applied Sciences, 11*(12), 5625. https://doi.org/10.3390/app11125625

Rizaldy, D., Ramadhita, N., Nadhifa, T., & Fidrianny, I. (2022). Mangosteen (*Garcinia mangostana* L.): Evaluation of in vitro antioxidant activities. *Pharmacognosy Journal, 14*(3), 633–640. https://doi.org/10.5530/pj.2022.14.82

Shikov, A., Obluchinskaya, E., Flisyuk, E., Терninко, И., Generalova, Y., & Pozharitskaya, O. (2022). The impact of natural deep eutectic solvents and extraction method on the co-extraction of trace metals from *Fucus vesiculosus*. *Marine Drugs, 20*(5), 324. https://doi.org/10.3390/md20050324

Sriwidodo, S., Pratama, R., Umar, A., Chaerunisa, A., Ambarwati, A., & Wathoni, N. (2022). Preparation of mangosteen peel extract microcapsules by fluidized bed spray drying for tableting: Enhancing solubility and antioxidant stability. *Antioxidants, 11*(7), 1331. https://doi.org/10.3390/antiox11071331

Sungpud, C., Panpipat, W., Yoon, A., & Chaijan, M. (2020). Ultrasonic-assisted virgin coconut oil-based extraction for maximizing polyphenol recovery and bioactivities of mangosteen peels. *Journal of Food Science and Technology, 57*(11), 4032–4043. https://doi.org/10.1007/s13197-020-04436-z

Tang, Z., Wang, Y., Huang, G., & Huang, H. (2023). Ultrasound-assisted extraction, analysis and antioxidant activity of polysaccharide from the rinds of *Garcinia mangostana* L. *Ultrasonics Sonochemistry, 97*, 106474. https://doi.org/10.1016/j.ultsonch.2023.106474

Teixeira, B., Vidigal, M., Júnior, B., Vieira, É., Martins, E., & Stringheta, P. (2023). Optimization, kinetic and phenomenological modeling of ultrasound-assisted extraction process of bioactive compounds from raspberries (*Rubus idaeus* L.). *Food Analytical Methods, 16*(4), 759–770. https://doi.org/10.1007/s12161-023-02462-z

Vo, T. P., Pham, N. D., Pham, T. V., Nguyen, H. Y., Vo, L. T. V., Tran, T. N. H., Tran, T. N., & Nguyen, D. Q. (2023). Green extraction of total phenolic and flavonoid contents from mangosteen (*Garcinia mangostana* L.) rind using natural deep eutectic solvents. *Heliyon, 9*, e14884. https://doi.org/10.1016/j.heliyon.2023.e14884

Xu, L., Liaqat, F., Khazi, M., Sun, J., & Zhu, D. (2024). Natural deep eutectic solvents-based green extraction of vanillin: Optimization, purification, and bioactivity assessment. *Frontiers in Nutrition, 10*, Article 1279552. https://doi.org/10.3389/fnut.2023.1279552

Yaneva, Z., Grozeva, N., Todorova, M., Kamenova-Nacheva, M., Staleva, P., Memdueva, N., & Tzanova, M. (2025). Comparison of the potential of "green" classical and natural deep eutectic solvents in the production of natural food colorant extracts from the roots of *Alkanna tinctoria* (L.). *Foods, 14*(4), 584. https://doi.org/10.3390/foods14040584

Yang, H., & Li, Q. (2022). Optimization of the extraction process and the antioxidant activity spectrum–effect relationship of *Angelica dahurica*. *Biomedical Chromatography, 36*(4), e5322. https://doi.org/10.1002/bmc.5322

Zahari, N., Chong, G., Abdullah, L., & Chua, B. (2020). Ultrasonic-assisted extraction (UAE) process on thymol concentration from *Plectranthus amboinicus* leaves: Kinetic modeling and optimization. *Processes, 8*(3), 322. https://doi.org/10.3390/pr8030322

Zhou, X., Da, X., Qu, J., & Shi-ming, X. (2024). Natural deep eutectic solvent-based ultrasound-assisted extraction of flavonoids from *Fagopyrum tataricum* bran. *Separations, 11*(5), 145. https://doi.org/10.3390/separations11050145